HYDRAULIC FRACTURING IN A NATURALLY FRACTURED RESERVOIR

L. K. Britt, Amoco Production Company
C. J. Hager, Amoco Production Company
J. W. Thompson, Schlumberger-Dowell

Abstract

Hydraulic fracturing of wells in naturally fractured reservoirs can differ dramatically from fracturing wells in conventional isotropic reservoirs. Fluid leakoff is the primary difference. In conventional reservoirs, fluid leakoff is controlled by reservoir matrix and fracture fluid parameters. The fluid leakoff rate in naturally fractured reservoirs is typically excessive and completely dominated by the natural fractures.

Historically, attempts to fracture-stimulate wells in naturally fractured reservoirs have been unsuccessful due to high leakoff rates and gel damage. The typical approach is to attempt to control the leakoff with larger pad volumes and solid fluid loss additives. This approach is not universally effective and can do more harm than good.

This paper presents several field examples of a fracture stimulation program performed on the naturally fractured Devonian carbonate of West Texas. Qualitative pressure decline analysis and net treating pressure interpretation techniques were utilized to evaluate the existence of natural fractures in the Devonian Formation. Quantitative techniques were utilized to assess the importance of the natural fractures to the fracturing process. This paper demonstrates that bottomhole pressure monitoring of fracture stimulations has benefits over conducting minifrac treatments in naturally fractured reservoirs. Finally, the results of this evaluation were used to redesign fracture treatments to ensure maximum productivity and minimize costs.

Introduction and Literature Review

Hydraulic fracturing in naturally fractured or fissured reservoirs can differ greatly from hydraulic fracturing in conventional reservoirs. In conventional reservoirs, fluid leakoff is dependent on matrix permeability, fluid viscosity, and reservoir fluid compressibility. Fluid leakoff in naturally fractured reservoirs is dominated by the natural fractures themselves. This fissure-dominated leakoff mechanism varies with stress or net pressure and, as a result, is less predictable. Because of this, treatments in naturally fractured reservoirs often terminate prematurely. As a result, it is critical that the existence of natural fractures be known prior to the hydraulic fracture treatment so that methods are employed to eliminate or at least minimize excessive leakoff. These methods have included the use of 100 mesh sand and/or silica flour and excessive fluid volumes and rates (i.e., live with it). Each of these techniques has had limited success.

Nolte and Smith[1] showed how natural fractures affected net treating pressures and established that treating pressures in excess of the critical pressure generally resulted in premature screenouts. In addition, they showed a qualitative method of identifying natural fractures by evaluating a log-log plot of net treating pressure versus pump time. Their work showed net pressure tends to flatten when excessive leakoff to the natural fractures occurs (i.e., the critical pressure is achieved). This qualitative interpretation technique has become an industry standard.

Nolte[2-6] presented diagnostic techniques for analyzing fracture behavior from pressure decline analysis. He showed diagnostic techniques for interpreting conventional and abnormal leakoff phenomena and qualitative techniques for identifying the existence of natural fractures. He further showed that the pressure decline function, G, for pressure-dependent leakoff is convex in character, and can be used as a diagnostic test of pressure-dependent leakoff.[7]

Numerous authors have presented results which showed that hydraulic fracturing in naturally fractured reservoirs can adversely impact well performance due to gel damage[8-11] and/or stress sensitivity.[12-15] These works highlight the detrimental effects of excessive leakoff in naturally fractured reservoirs.

Mukherjee[16] showed the stress-sensitive nature of the fluid leakoff and proposed methodology to handle fluid leakoff as a function of net treating pressure. Warpinski[17] showed that the fluid leakoff to natural fracture systems can be as much as 50 times greater than matrix leakoff. He further presented the successful application of 100 mesh sand as a fluid loss additive in naturally fractured reservoirs to minimize these detrimental effects, as did Northcutt et al.[18]

Cramer[19] addressed the excessive fluid loss to natural fractures by reducing net treating pressure, thereby minimizing the leakoff into the fracture system.

This paper shows the interpretation of treating pressure and pressure decline data from the naturally fractured Devonian Formation of West Texas. Methods used to interpret the hydraulic fracturing process and techniques to minimize excessive leakoff to natural fractures are presented. The paper shows that by understanding the nature of the natural fractures, fracture treatments can be optimized to maximize postfrac well performance while minimizing treatment costs.

Geologic Summary

The lower Devonian (Lockovian to Pragian) Thirtyone Formation of West Texas is host to major accumulations of oil, gas and condensate. Figure 1 shows a stratigraphic column highlighting the Thirtyone Formation which lies between the Devonian age Woodford shale and the Silurian age Wristen Formation. In eastern Ector and western Midland counties, several major retrograde gas-condensate reservoirs occur in the Thirtyone Formation along a northwest-southeast trending structural anticline. This anticline is bounded on the east by a near-vertical fault system, locally with up to 400 ft of dip-slip displacement.

Fields along this productive Devonian trend include (from south to north) Pegasus, Dora Roberts, Headlee and Ratliff Ranch. Subsea depths to the top of the Devonian along this trend range from approximately -8,200 to -9,500 ft. Figure 2 shows a map of the northern portion of the Devonian trend and highlights the wells reviewed in this paper.

Productive rock in the Thirtyone Formation consists of fine-grained, laminated chert and cherty limestone, and horizontal- to cross-laminated skeletal grainstone and packstone. Chert nodules and layers occur scattered throughout the reservoir. The porosity in the main producing interval in the Headlee Field is mostly secondary (leached bryozoans, leached lime mud and fractures) with an average porosity for this interval approaching 5%. Porosity in the main producing interval appears to be best developed on top of the structure. Natural fractures in the carbonate are the primary permeability conduits. Fracturing may be enhanced in the Headlee Field in those areas proximal to the fault system along the eastern flank of the field.

The productive rock from the Ratliff Ranch was deposited in a similar environment. However, reservoir quality and average porosity are generally poorer than the fields to the south. The main permeability conduits probably are microfractures in the carbonate. The lower reservoir quality of the Ratliff Ranch is likely due to: (1) lower depositional porosities and higher lime mud content, (2) less leaching of the lime mud and bryozoans during burial diagenesis, or (3) less fracturing of the reservoir rock during late deformation. Figure 3 shows a type log of the Devonian Formation in the area. This figure shows a gamma ray and porosity log highlighting the productive interval.

Figure 4 shows a geomechanical type log comparing long-spaced digital sonic log (LSDS) derived rock properties and triaxial laboratory tests. As shown, fairly good agreement exists between the LSDS and laboratory derived Young's Modulus and Poisson's Ratio. Further, the average Young's Modulus of 9.6 million psi and Poisson's Ratio of 0.335 (triaxial tests) are fairly typical of West Texas carbonate formations.[21] This data was used to develop fracture stimulation designs for wells in the Devonian trend.

Fracture Design Considerations

Numerous design parameters were considered in engineering treatments for hydraulically fracturing the area under investigation. Several parametric studies were conducted to examine the influence of fracture half-length (x_f), fracture conductivity (k_fw), fracture height growth (Ht) and closure pressure (P_c) on net pressure value (NPV). The results of the parametric studies can be seen in Figures 5 and 6.

Figure 5 shows the influence of closure pressure on NPV and provides valuable insight towards selecting the correct proppant. Two types of intermediate strength proppant (ISP) were being considered, a precured RCP and a ceramic proppant. The ceramic proppant had a significantly higher permeability (2 X @ 8,000 psi) than the RCP; however, the cost of the ceramic proppant was approximately 60% higher. The results form Figure 5 show that the precured RCP resulted in a higher NPV than the ceramic proppant at all fracture lengths and closure stresses presented. Therefore, the use of the precured RCP in this formation was considered more optimum.

The effect of fracture height growth was also a critical factor in the fracture treatment design. Based on core data and sonic log information, it was suspected that no significant barriers existed which would limit the fracture height growth to within the zone of interest. Hence, the design of the optimum fracture half-length could not be performed without considering the possibility of excessive height growth. Figure 6 shows the results of this study and suggests that fracture height growth does not become a limiting factor until fracture half-lengths exceed 300 ft. Also shown is that the incremental differences of NPV for various fracture heights become more pronounced with longer fracture lengths.

The fracture treatments were justified through economics and were engineered using the information obtained from the sensitivity runs, and experience gained from each fracture treatment. Associated risk factors were also taken into consideration. In general, the fracture treatments were designed for a fracture half-length of around 300 ft with a fracture conductivity of around 240 mdft. The fracturing treatments typically involved pumping approximately 200,000 lb of a 20/40 precured RCP using a delayed borate cross-linked fluid. Table 1 gives a more specific description of the treatment designs for the wells of interest to this paper.

In addition to the fracture optimization studies, a review of fracture stimulations in wells in the Devonian Formation[20] was conducted. This review indicated that premature job terminations were fairly common and when coupled with the geologic description, raised concerns regarding the existence and effects of natural fractures on treatment execution. As a result, preparations were made to pump 100 mesh sand to control potential fluid loss to the natural fracture system and natural fracture evaluation techniques were reviewed.

Natural Fracture Evaluation Technique

Figure 7 shows a series of drawings which depict the interrelationship between the hydraulic fracture and the natural fractures. The first depiction is the creation of a hydraulic fracture when the fracture treating pressure is less than that required to open the natural fractures. During this time frame, the fluid loss is typical of a conventional reservoir, and thereby governed by reservoir pressure, compressibility, fluid viscosity and relative permeability. Depiction 2 shows the hydraulic fracture when the fracture treating pressure is in excess of the pressure necessary to open or widen the natural fractures. At this time, fluid loss is becoming excessive and loss to the natural fracture system begins to dominate. Depiction 3 shows the usual result of the excessive leakoff shown by Depiction 2, dehydration of the slurry and a screen-out.

As shown in Figure 7, ability to control fluid loss to natural fractures is dependent on knowing at what stress the natural fractures opens. Knowing this stress level, the net treating pressure can be monitored to improve our understanding of the effects of the opening of natural fractures on the fracturing process. Figure 8 shows a plot of net treating pressure (treating pressure - fracture closure pressure) which highlights the slope interpretation technique proposed by Nolte and Smith.[1] This plot is typically used to identify fracture geometry. Mode I character, for example, shows an increasing net pressure typical of a confined height extending fracture, while Mode IV shows net treating pressure character typical of fracture height growth. In addition to identifying the fracture geometry, this plot can be used to identify when the natural fractures are open, as shown by Mode II. During this time, the net treating pressure flattens as the opening of the natural fractures causes excessive leakoff and tends to regulate pressure.

Another technique which can be used to qualitatively interpret the existence of natural fractures is the use of pressure decline analysis. Figure 9 shows a plot of pressure change versus the pressure decline function, G, which contrasts the ideal or typical pressure decline following a hydraulic fracture treatment to the pressure decline associated with pressure dependent fluid loss such as natural fractures. As shown, in the presence of open natural fractures the pressure decline function exhibits a concave up character.

Subsequent sections detail several case histories which use the interpretation techniques to prove the existence of natural fractures and test the ability to control leakoff.

Case Histories

Well A

The initial well in the Devonian fracture program, shown as Well A in Figure 2, was on the southeastern periphery of the Devonian Field area. A foamed fracture stimulation had been performed with little success and a refracture stimulation was planned. A minifrac treatment was performed to aid treatment design. Figure 10, a plot of pressure and rate versus time for the Well A minfrac, shows that the minifrac was pumped at 45 bpm and achieved a treating pressure of nearly 7,000 psi. Following the minifrac, pressure declined to nearly 4,000 psi during the 50-minute monitoring period. Note that the treating pressure rose throughout the minifrac treatment period indicative of fracture containment. Also note that no flattening occurred, raising questions about the existence of natural fractures, as compared to the pump times in Wells B and C necessary to open the fissures; however, it is possible the fissures do exist in Well A but the minifrac was not large enough to dilate them.

An analysis of the minifrac pressure decline was performed using a square root of time and G-function plot as illustrated by Figures 11 and 12, respectively. From the analysis, closure pressure and the treatment fluid efficiency were determined at 5,800 psi and 38%, respectively. Examining the G-function plot, as illustrated in Figures 12 and 13, shows no evidence of a pressure-dependent leakoff environment. This information further supports that no natural fractures were present during the minifrac.

No evidence of natural fractures was seen during the minifrac. However, because the minifrac volume was small and the treating pressure increased throughout, concern still existed that the natural fractures would be seen during larger treatments at higher treating pressures. As a result, 100 mesh sand was used as a fluid loss additive during the pad fraction as a safety factor. The treatment specifics for Well A are shown in Table 1.

Following the treatment of Well A, the next two wells were fracture stimulated in a similar manner. Each of the stimulations had anomalous surface treating pressure data. As a result, the fracture stimulations on subsequent Wells B and C were performed while the bottomhole pressure was recorded. A pressure gauge was placed in a pup joint in the bottom of the well to aid understanding of the treatment pressures.

Well B

Well B was fracture stimulated with 225,000 gallons of 30-40 lb/1,000 gal Borate at a rate of 60 bpm, as shown in Table 1. Figure 14 shows a plot of pressure and rate versus time for the treatment. Analysis of this figure shows that treating pressures are indicative of fracture containment. Figure 15 presents a Nolte-Smith plot of net pressure, which shows the treating pressure increasing for nearly 30 min (to approximately 1,000 psi), at which time the treating pressure leveled off until the end of the treatment. Qualitatively, natural fracture leakoff is indicated after 30 minutes of pumping. Figures 16 and 17 show plots of pressure versus square root of time and G-function, respectively. Interpretation of the pressure decline data indicates a fracture closure pressure of approximately 6,890 psi (closure on proppant) and a final net pressure of 1,031 psi. Further, early time pressure decline exhibited a concave upward behavior. Closer inspection of this early time data, shown in Figure 18, indicates a rapid pressure decline from 7,927 psi to approximately 7,630 psi where the pressure decline becomes linear. This early time pressure decline is characteristic of pressure-dependent leakoff such as exists with natural fractures.

Well C

Well C was fracture stimulated with 145,000 gallons at a rate of 40 bpm, as summarized in Table 1. Figure 19 shows a plot of pressure and rate versus time for the treatment on Well C. As shown, the treating pressure increased throughout the treatment, though from approximately 45 minutes, the rate of pressure rise slowed dramatically. This effect is clearly illustrated by the Nolte-Smith net treating pressure plot in Figure 20. The net treating pressure increasing until about 40 minutes (1,000 psi), at which time net treating pressure flattened through the end of the treatment.

Figures 21 and 22 show plots of pressure versus square root of time and G-Function, respectively. Pressure decline interpretation of these plots indicates a closure pressure of approximately 6,675 psi (closure on proppant) and a final net treating pressure of 1,126 psi. Additionally, the early time pressure decline data, shown in Figure 23, suggests evidence of natural fractures.

Another use of the pressure decline analysis is to develop an understanding of the character of the hydraulic fracture. To develop this understanding, the postfracture pressure decline data from several Devonian wells were evaluated to identify the hydraulic fracture and fissure closures and treatment fluid efficiencies. Recognize that the data from Wells B and C represent postfracture treatment data and that fracture closure was on proppant. As a result, closure was several hundred psi above actual hydraulic fracture closure and closed faster than if it had been unpropped. The treatment fluid efficiency required correction for closure on proppant. Table 2 summarizes the results of this analysis and includes treatment fluid efficiency for the fracture closure.

Table 3 summarizes the results for fissure closure. The efficiency, e_f, is corrected for the closure on proppant, while the efficiency, e_f^*, reported in Table 3 represents the fluid efficiency based on natural fracture closure. For design purposes, the efficiency based on natural fracture closures was used for Wells B and C. The proppant closure corrected efficiency should only be used for design when leakoff to natural fractures is not dominating. These results indicate that hydraulic fracture closure occurred at pressures on the order of 6,500-6,600 psi which is consistent with the natural fractures opening at 7,500-7,600 psi. This is also consistent with pressure regulated net treating pressures due to the opening of natural fractures of 1,000 psi.

A further look at the pressure decline data shows that the pressure required to open (or close) the natural fractures can be quantitatively determined. Referencing again Figure 23, note that the pressure at which the concave character first exhibits linear behavior is at a pressure of 7,500 psi, while from Figure 18, a linear trend is established at nearly 7,630 psi. Thus, if treating pressures less than 7,500-7,600 psi can be achieved, no excess fluid loss should occur, as the stress-dependent natural fractures will not have opened. Table 3 summarizes the pressure required to open the natural fractures for the Devonian wells evaluated.

Well D

Both qualitative and quantitative interpretation methods were applied to the data from Wells B and C to assess the existence of natural fractures and stresses at which they dominate the hydraulic fracturing process. This analysis suggests that by keeping net treating pressure below 800 psi, a fracture stimulation could be performed without incurring excessive leakoff to the natural fractures. Understanding that we have some, albeit limited, control over the net fracture pressure for a contained fracture which is described by

$$P_{net} \sim \left(\frac{E^{3/4}}{H}\right)(\mu Q L)^{\frac{1}{4}}. \tag{1}$$

Investigation of Equation 1 shows that by controlling pump rate, Q, and fracture fluid viscosity, μ, we can potentially keep the net treating pressure below the threshold pressure required to open the natural fractures. For example, by cutting the rate orviscosity at which the treatment is pumped in half, net pressure can be reduced by nearly 20%. For the jobs in the Devonian Formation, a minimum of 300 psi drop in net pressure is needed in order to stay under the threshold pressure of the natural fractures. A treating pressure reduction of this magnitude may be sufficient to allow the treatment to be pumped to completion without dilating the natural fractures. From a cost perspective, a reduction in pump rate will reduce the hydraulic horsepower requirements, and staying below the pressure required to open the natural fractures will eliminate the need for 100 mesh sand as a fluid loss additive and allow a reduced pad fraction to be pumped. The treatment parameters and cost savings from these modifications are shown in Tables 1 and 4.

Table 4 shows a comparison of the fracture design pumped in Well C to a modified design based on the reduced net pressure treatment pumped in Well D. As shown, a cost savings of $64,000, which represents a treatment cost reduction of nearly 40% over previous treatments. This cost reduction was obtained with no impact on performance, as the propped fracture length and conductivity remained relatively unchanged. The treatment in Well D was pumped successfully. Bottomhole pressure was recorded in Well D in a similar manner as previous wells; however, the bottomhole pressure gauges failed. Analysis of surface treating pressure indicated that we achieved our objective and successfully reduced treating pressure.

Post-Appraisal

The production from this reservoir is a retrograde gas condensate. The wet gas typically contains 8.6 gal of NGLs per MCF of wet gas. The Gas to Oil Ratio at the separator usually starts at 4,000 scf/stb and slowly increases to a maximum 32,000 scf/stb, depending on the reservoir pressure relative to the dew point.

The complex reservoir fluid system makes it difficult to evaluate fracture effectiveness through postfracture evaluation of performance. In addition, liquid loading results in erratic well productivity. Table 5 summarizes the performance of the wells from the Devonian fracture program. As shown, prefrac performance varied from Well A which produced 190 boepd to Well D which was unable to produce. Postfracture production had similar variability. Also note that Wells B and C produced at higher watercut than the other fracture-stimulated Devonian wells. The water production is believed to come from a lower Devonian horizon. Reduction of net treating pressure by reducing treatment rate and fluid viscosity (Equation 1) may also minimize the chances of communicating with the water zone by minimizing height growth.

Conclusions

1. Treating pressure and pressure decline analysis techniques are effective for identifying the existence of natural fractures.
2. Control of net treating pressure through reduction in treatment rate and fluid viscosity can effectively minimize leakoff to natural fractures.
3. Control of net treating pressure in naturally fractured reservoirs can dramatically reduce treatment costs.
4. Bottomhole pressure monitoring of the main fracture stimulation (in lieu of conducting a minifrac) should be considered in naturally fractured reservoirs to enable the identification of these fracture systems.

Acknowledgment

The authors wish to thank Amoco Production Company and Schlumberger-Dowell for permission to publish this paper. In addition, we would like to thank Thal Mcguinness and Tad Smith for aid in understanding the geology of the Devonian area.

Nomenclature

e_f	= efficiency based on fracture closure corrected for closure on proppant
e_f^*	= efficiency based on fissure closure
$k_f w$	= fracture conductivity in mdft
H_t	= fracture height in feet
x_f	= fracture half-length in feet
P_C	= fracture closure pressure in psia
P_C^*	= fissure closure pressure in psia
NPV	= Net Present Value in dollars
RCP	= Resin Coated Proppant
ISP	= Intermediate Strength Proppant
P_{net}	= Fracture Net Treating Pressure in psia
P_{net}^*	= Fissure Net Treating Pressure in psia
E	= Young's Modulus in 1/psia
μ	= fracture fluid viscosity in cp
Q	= pump rate in bpm
BHP	= Bottomhole Pressure in psia
L	= fracture length in feet
P_{isip}	= Pressure at initial shut-in in psia
N/A	= Not Applicable

References

1. Nolte, K. G. and Smith, M. B.: "Interpretation of Fracturing Pressures," paper SPE 8297 presented at the 54th Annual Technical Conference and Exhibition, Las Vegas, NV, Sept. 1979.
2. Nolte, K. G.: "Determination of Fracture Parameters from Fracturing Pressure Decline," SPE 8341, Las Vegas, NV, Sept. 1979.

3. Nolte, K. G.: "Principles of Fracture Design Based on Pressure Analysis, **SPE Production Engineering**, pp. 22-30, Feb. 1988.

4. Nolte, K. G.: "A General Analysis of Fracturing Pressure Decline with Application to Three Models," **SPE Formation Evaluation**, Vol. 1, pp. 571-583, Dec. 1986.

5. Nolte, K. G.: "Fracturing Pressure Analysis: Deviations from Ideal Assumptions," SPE 20704, presented at the SPE Annual Technical Conference, New Orleans, LA, 1990.

6. Nolte, K. G., Mack, M. G., and Lie, W. L.: "A Systematic Method for Applying Fracturing Pressure Decline: Part 1," SPE 25845, presented at the SPE Low Permeability Symposium, Denver, CO, April 1991.

7. Warpinski, N. R.: "Hydraulic Fracturing in Tight Fissured Media," NMT 890020, presented at the Centennial Symposium of Petroleum Technology into the Second Century at New Mexico Tech., Socorro, NM, Oct. 1989.

8. Branagan, P. T., Cipolla, C. L., Lee, S. J. and Yan, L.: "Case History of Hydraulic Fracture Performance in the Naturally Fractured Paludal Zone: The Transitory Effects of Damage," SPE 16397, presented at the SPE Low PErmeability Reservoirs Symposium, Denver, CO, May 1987.

9. Cipolla, C. L., Branagan, P. T. and Lee, S. J.: "Fracture Design Considerations in Naturally Fractured Reservoirs," SPE 17607, presented at the SPE International Meeting on Petroleum Engineering, Tianjin, China, Nov. 1988.

10. Palmer, I. D., Fryar, R. T., Tumino, K. A. and Puri, R.: "Comparison Between Gel-Fracture and Water Fracture Stimulations in Black Warrior Basin," SPE 23415, presented at the 1991 Coalbed Methane Symposium, Tuscaloosa, AL, May 1991.

11. Puri, R., King, G. E. and Palmer, I. D.: "Damage to Coal Permeability During Hydraulic Fracturing," SPE 21813, presented at the SPE Low Permeability Reservoirs Symposium, Denver, CO, April 1991.

12. Palmer, I. D.: "Induced Stresses Due to Propped Hydraulic Fracture in Coalbed Methane Wells," SPE 25861, presented at the SPE Low Permeability Reservoirs Symposium, Denver, CO, April 1993.

13. Buchsteiner, H. Warpinski, N. R., Economides, M. J.: "Stress-Induced Permeability Reduction in Fissured Reservoirs," SPE 26513, presented at the 68th Annual Technical Conference and Exhibition of the Society of Petroleum Engineers, Houston, TX, Oct. 1993.

14. Fatt, I. and Davis, T. H.: "The Reduction in Permeability with Overburden Pressure," Trans., AIME, 195 (1952), 329.

15. Kranz, R. L., Frankel, A. D., Engelder, T. and Scholz, C. H.: "The Permeability of Whole and Jointed Barre Granite," Int. J. of Rock Mechanics, Min. Science & Geoph. Abstracts, 16 (1979), pp. 225-234.

16. Mukherjee, H., Larkin, S. and Kordziel, W.: "Extension of Fracture Pressure Decline Curve Analysis to Fissured Formations," SPE 21872, presented at the SPE Low Permeability Reservoirs Symposium, Denver, CO, April 1991.

17. Warpinski, N. R.: "Dual Leakoff Behavior in Hydraulic Fracturing of Tight, Lenticular Gas Sands," SPE 18259, presented at the 63rd Annual Technical Conference and Exhibition of the Society of Petroleum Engineers, Houston, TX, Oct. 2-5, 1933.

18. Northcutt, J. C., Robertson, C. J., Hannah, R. R.: "State-of-the-Art Fracture Stimulation of the Upper Morrow Formation in the Anadarko Basin," SPE 18260, presented at the SPE 63rd Annual Technical Conference and Exhibition, Houston, TX, Oct. 1988.

19. Cramer, D. D.: "Treating Pressure Analysis in The Bakken Formation," SPE 21820, presented at the Low Permeability Reservoirs Symposium, Denver, CO, April 1991.

20. Olson, K. E.: "A Case Study of Hydraulically Refractured Wells in the Devonian Formation, Crane, County, Texas," SPE 22834 presented at the 66th Annual Technical Conference, Dallas, TX, October 6-9, 1991.

21. Britt, L. K., Larson, M. J.: "Fracture Characterization of Multilayered Reservoirs," SPE 15511, presented at the 61st Annual Technical Conference, New Orleans, LA, Oct. 5-8, 1986.

Table 1 - Fracturing Treatment Design Description

Well	Fluid Mgals	Polymer Load #/Mgal	Pad %	Rate bpm	Prop Conc. ppg	Prop, Mlbs	100 Mesh Mlbs	x_f ft	$k_f w$ mdft
A	139	40	63.8	45	2-8	200	13	720	235
B	225	40 & 30	60.6	60	2-6	300	13	400	240
C	145	40	61.7	40	2-6	200	12.6	270	230
D	90	30 & 25	40.4	20	2-6	200	0	290	184

Table 2 - Evaluation of Pressure Decline Data

Well	P_{isip} (psia)	P_C (psia)	P_{net} (psia)	e_f	Slurry Volume (Mgals)
A	6542	5800	770	.38	37
B	7917	6890	1031	.59	236
C	7812	6675	1126	.53	157

Table 3

Well	P_{isip} (psia)	P_C^* (psia)	P_{net}^* (psia)	e_f^*	Slurry Volume (Mgals)
A	6542	N/A	N/A	N/A	37
B	7917	7630	287	.23	236
C	7812	7500	312	.18	157

Table 4 - Fracture Treatment Designs

Well C			Well D		
Fluid Volume (Mgals)	**Prop Conc. (ppg)**	**Prop Type**	**Fluid Volume(Mgals)**	**Prop Conc. (ppg)**	**Prop Type**
30	0.0				
35	0.5	100 Mesh			
30	0.0		40	0	
10	2.0	20/40 RCP	10	2	20/40 RCP
30	4.0	20/40 RCP	30	4	20/40 RCP
10	6.0	20/40 RCP	10	6	20/40 RCP
Pump Rate 40 bpm			Pump Rate 20 bpm		
Cost $159,000			Cost $96,000		

Table 5 - Devonian Performance Appraisal

Well	Prefrac Rate (boepd)	Maximum Postfrac Rate (boepd)	Stabilized Postfrac Rate (boepd)	Watercut (Percent)
A	190	700	400	15
-	New Well	300	200	15
-	13	100	70	15
B	New Well	400	200	25
C	New Well	220	80	55
D	0	130	100	15

Cisco	Penn.
Canyon	
Strawn	
Atoka	
Morrow	
Barnett	Miss.
Mississippian Lst.	
Woodford	Dev.
Thirtyone	
Wristen	Sil.
Fusselman	
Montoya	Ord.
Simpson Grp.	
Ellenberger	
Moore Hollow Grp.	

Figure 1 - Stratigraphic Column

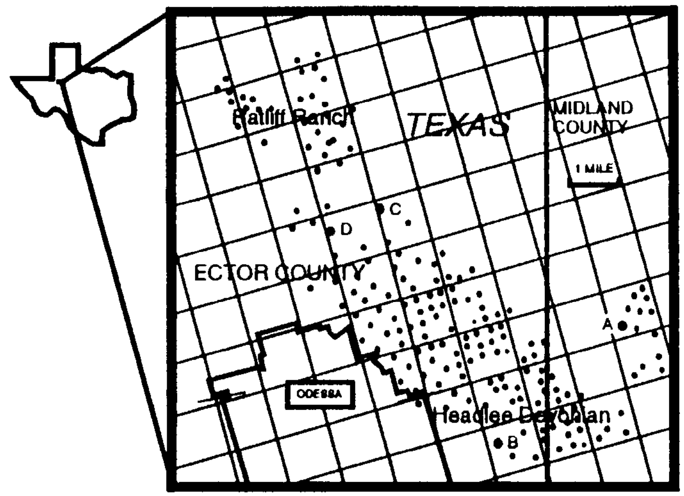

Figure 2 - Location Map

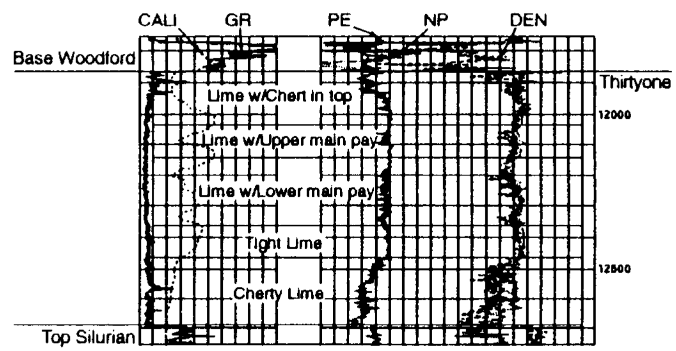

Figure 3 - Devonian Type Log

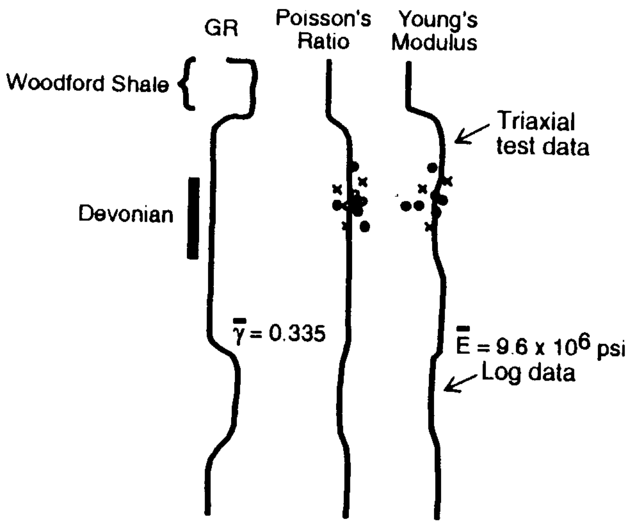

Figure 4 - Geomechanical Type Log

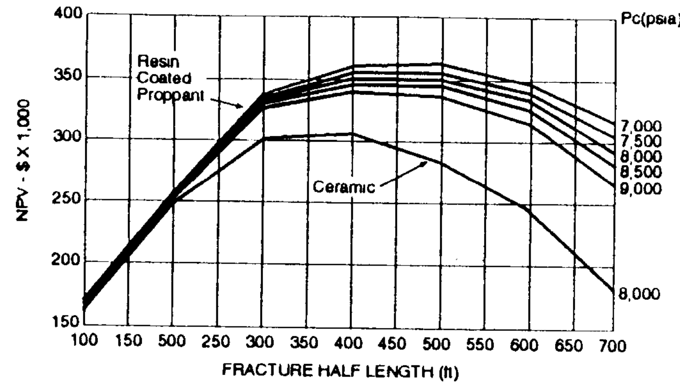

Figure 5 - NPV Proppant Sensitivity

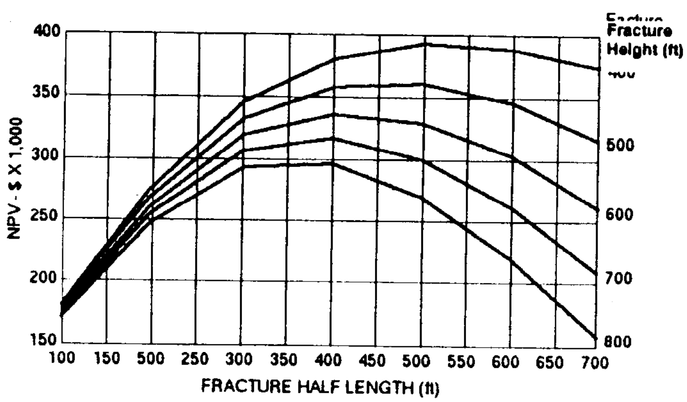

Figure 6 - Fracture Height Sensitivity

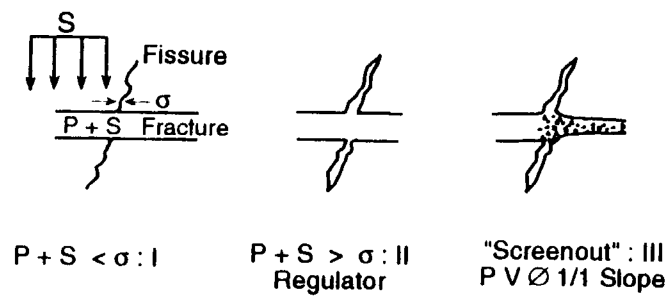

Figure 7 -Natural Fracture Depiction

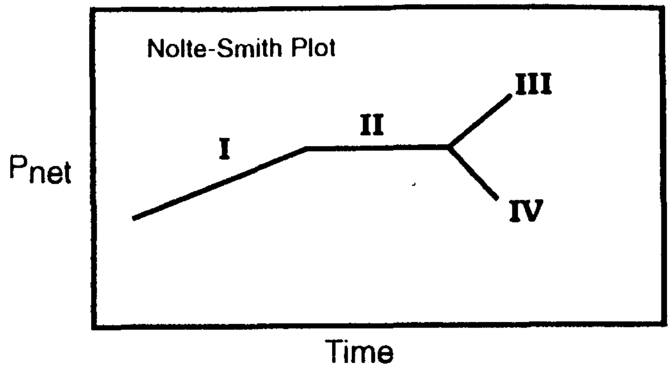

I Contained Height - Unrestricted Extension
II Stable Growth/Natural Fracture Opening
III Restricted Extension (Screenout)
IV Unstable Height Growth

Figure 8 - Nolte-Smith Interpretation Guide

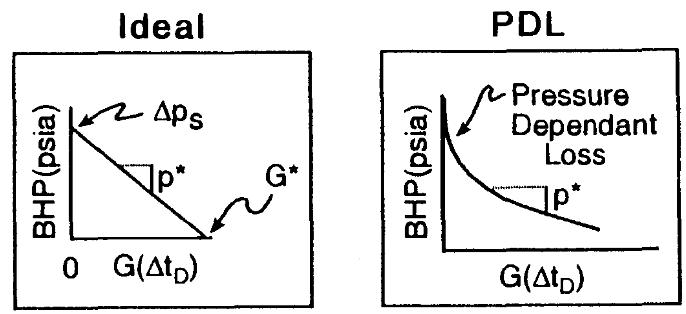

Figure 9 - Pressure Decline Interpretation Guide

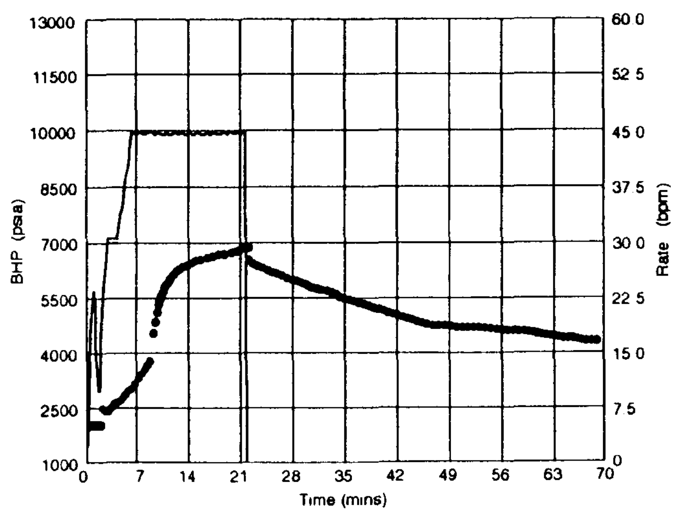

Figure 10 - Well A Minifrac Treatment

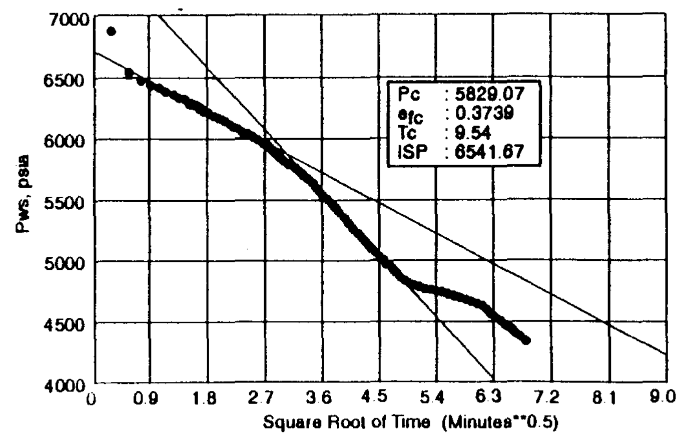

Figure 11 - Well A Minifrac Square Root of Time

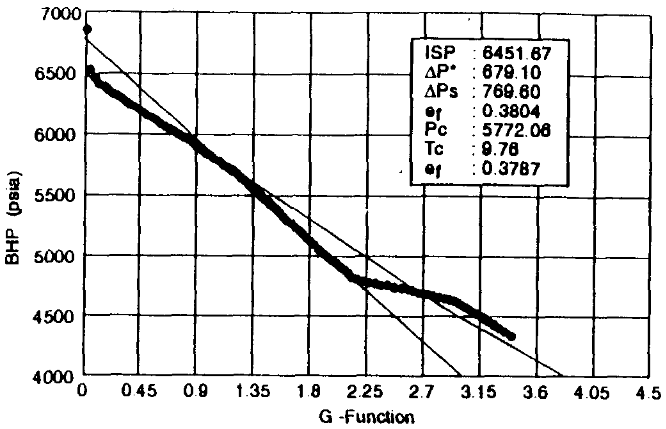

Figure 12 - Well A Minifrac G-Function

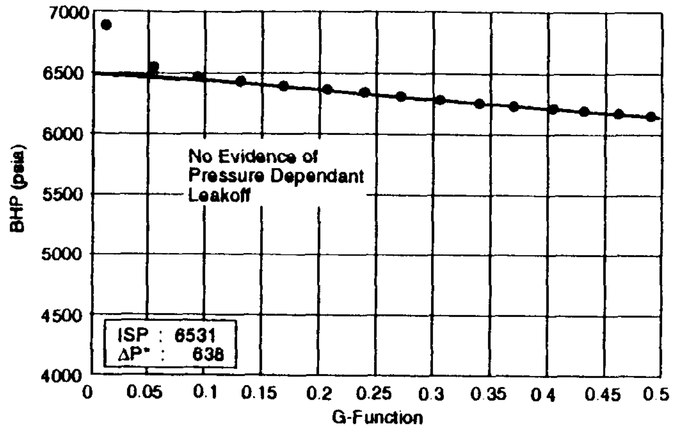

Figure 13 - Well A Minifrac Natural Fracture Evaluation

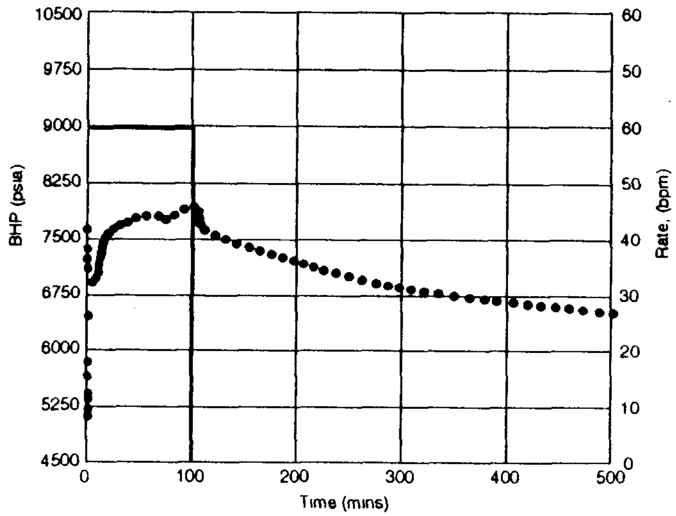

Figure 14 - Well B Fracture Treatment

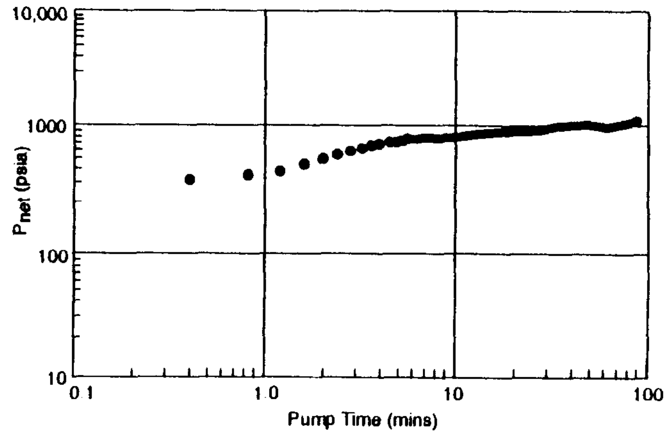

Figure 15 - Well B Fracture Nolte-Smith Plot

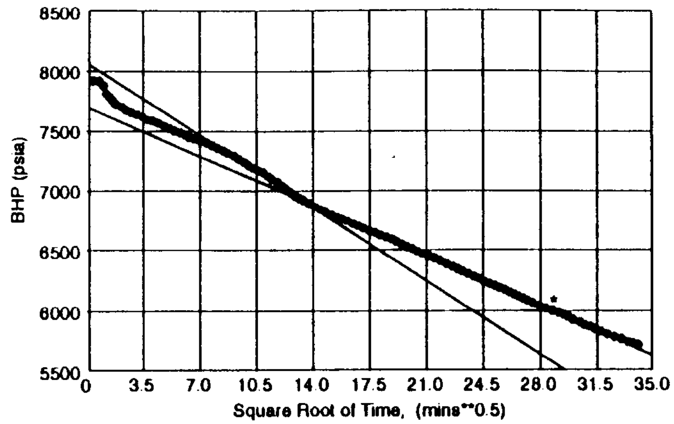

Figure 16 - Well B Fracture Square Root of Time

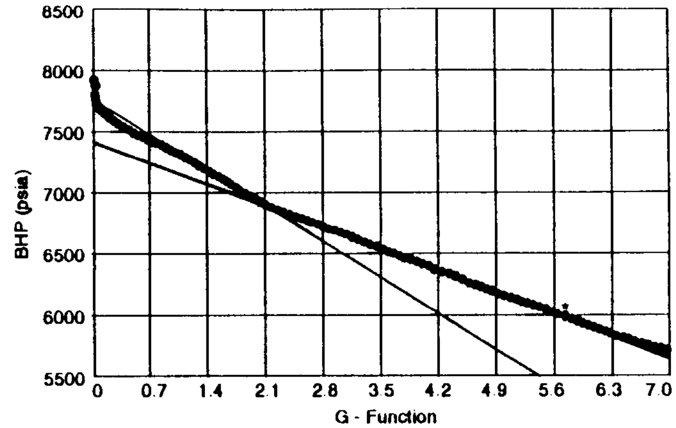

Figure 17 - Well B Fracture G-Function

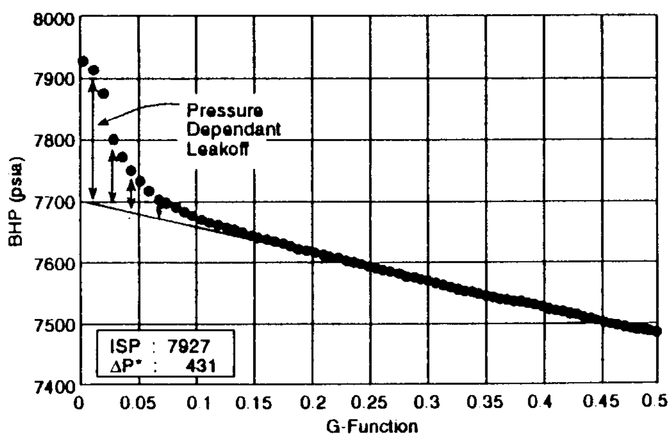

Figure 18 - Well B Fracture Natural Fracture Evaluation

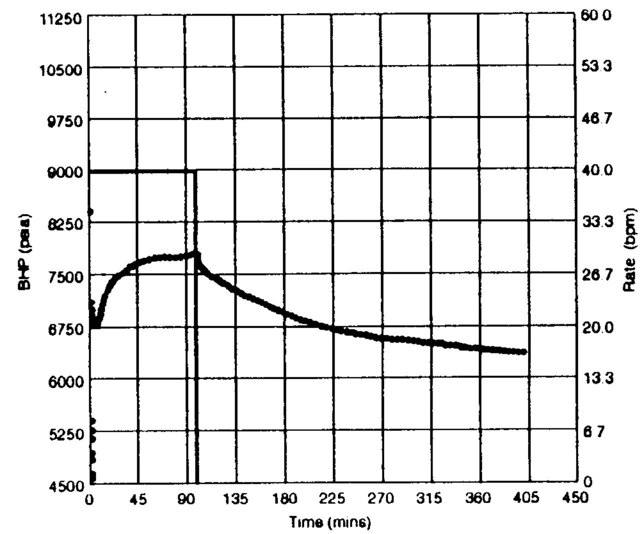

Figure 19 - Well C Fracture Treatment

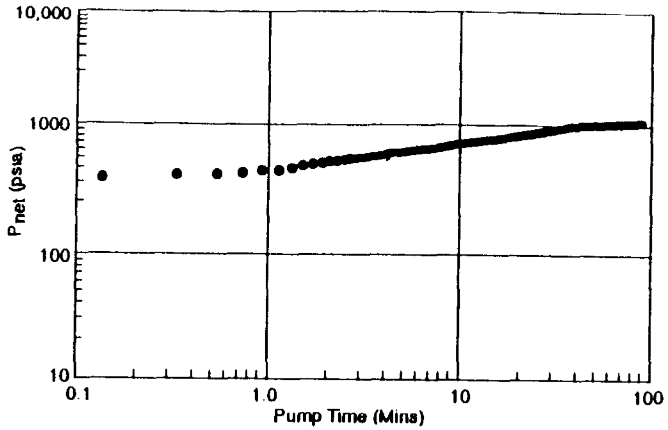

Figure 20 - Well C Fracture Nolte-Smith Plot

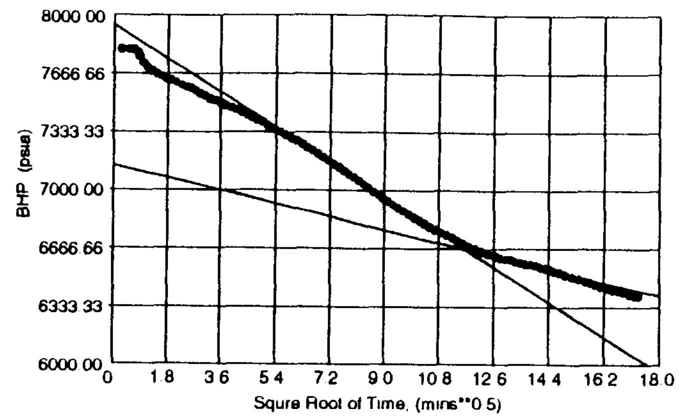

Figure 21 - Well C Fracture Square Root of Time

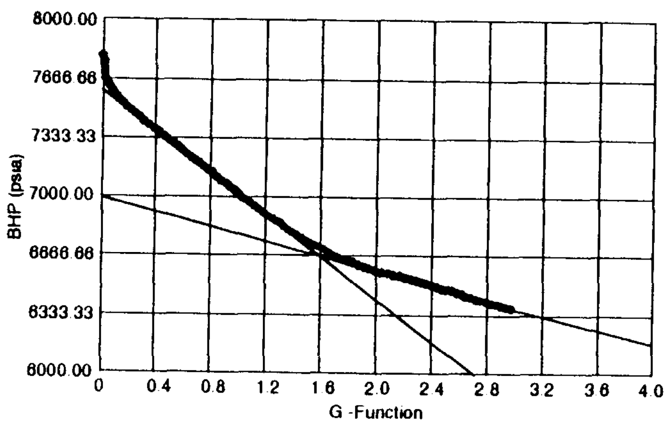

Figure 22 - Well C Fracture G-Function

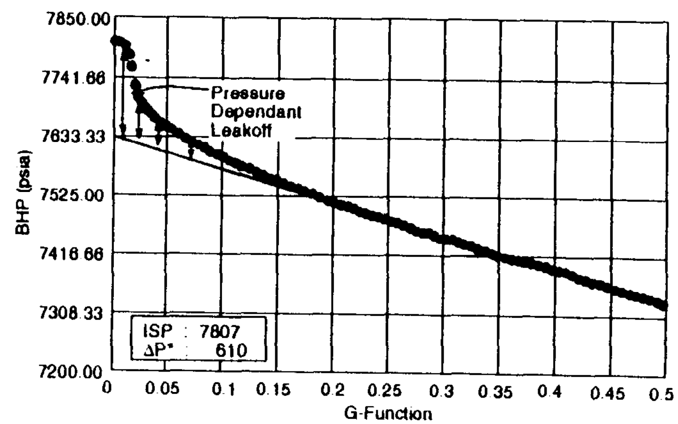

Figure 23 - Well C Fracture Natural Fracture Evaluation